



## A comparison of in situ bottom pressure array measurements with GRACE estimates in the Kuroshio Extension

Jae-Hun Park,<sup>1</sup> D. Randolph Watts,<sup>1</sup> Kathleen A. Donohue,<sup>1</sup> and Steven R. Jayne<sup>2</sup>

Received 22 May 2008; revised 24 July 2008; accepted 7 August 2008; published 10 September 2008.

[1] Ocean bottom pressure estimates from Gravity Recovery and Climate Experiment (GRACE) have been validated by comparisons with an array of in situ bottom pressure measurements. The 600 km by 600 km array comprised 46 bottom pressure sensors that were part of the Kuroshio Extension System Study (KESS). Validations in other ocean regions have been limited by available data to pointwise bottom pressure measurements. Spatially-averaged monthly-mean bottom pressure over the KESS array is highly correlated with GRACE bottom pressure estimated at the center of the array. The correlations are nearly equally high for three standard choices of spatial smoothing radius applied to GRACE estimates, 300, 500, and 750 km. In contrast, pointwise comparisons between GRACE and individual bottom pressures are high or low in sub-regions of KESS, depending partially upon the local variance of deep mesoscale eddies whose energetic length scales are shorter than 300 km. KESS is a suitable validation experiment for the GRACE estimates at monthly scales with 300 to 750 km spatial radius of smoothing. **Citation:** Park, J.-H., D. R. Watts, K. A. Donohue, and S. R. Jayne (2008), A comparison of in situ bottom pressure array measurements with GRACE estimates in the Kuroshio Extension, *Geophys. Res. Lett.*, *35*, L17601, doi:10.1029/2008GL034778.

### 1. Introduction

[2] The Gravity Recovery and Climate Experiment (GRACE) mission, launched in March 2002, measures global gravity fields at monthly intervals [Tapley *et al.*, 2004]. In the ocean, temporal changes in GRACE gravity fields arise from water mass redistribution due to atmospheric forcing, ocean currents, and net fresh water fluxes such as from evaporation, precipitation, river run-off, or ice melting. Satellite altimeters measure sea surface height which includes both steric and mass-loading components. The former are associated with subsurface temperature and salinity changes causing expansion or contraction of the water column and do not contribute to mass loading. One of the scientific objectives of the GRACE mission is to produce high-quality ocean mass-loading estimates that can be used in conjunction with altimeter sea surface height estimates to derive the steric sea surface height signal

[Jayne *et al.*, 2003]. GRACE is poised to benefit climate change studies and ocean model validations [e.g., Chambers, 2006b].

[3] To evaluate GRACE estimates in the ocean, a few comparison studies have been done between GRACE-derived and in situ ocean bottom pressure ( $P_{bot}$ ) [e.g., Kanzow *et al.*, 2005; Rietbroek *et al.*, 2006; Munekane, 2007]. Munekane [2007] notes that comparison between GRACE-derived  $P_{bot}$  and sparsely-distributed pointwise in situ  $P_{bot}$  could lead to low correlations because GRACE measures spatially-smoothed mass variations [e.g., Kanzow *et al.*, 2005]. The Kuroshio Extension System Study (KESS) experiment offers a unique opportunity to compare the GRACE  $P_{bot}$  estimates with spatially-averaged in situ  $P_{bot}$  measurements since the KESS array, composed of 46  $P_{bot}$  sensors, covered a wide area of about 600 km  $\times$  600 km as shown in Figure 1. Here we compare GRACE  $P_{bot}$  estimates produced by Chambers [2006a] with the KESS in situ  $P_{bot}$  array measurements. We will show that GRACE  $P_{bot}$  estimated at the center of the array correlates highly with the spatially-averaged (array-averaged) monthly-mean  $P_{bot}$ . Within the array, pointwise correlations between individual KESS records and GRACE can be low. In particular, the presence of short-wavelength (<300 km) mesoscale  $P_{bot}$  components reduce local correlations.

### 2. Data

[4] We use GRACE  $P_{bot}$  estimates obtained from the GRACE Tellus Web site (<http://gracetellus.jpl.nasa.gov/data/mass/>), which provides  $1^\circ \times 1^\circ$  monthly GRACE  $P_{bot}$  fields in terms of equivalent water thickness processed using the Release-04 data sets from Center for Space Research (CSR), Jet Propulsion Laboratory (JPL), and GeoForschungsZentrum Potsdam (GFZ). Details of the GRACE  $P_{bot}$  estimates are given by Chambers [2006a]. In this study, we evaluate altogether nine data products with 300-, 500-, and 750-km Gaussian smoothing radii ( $R$ ) from the three different institutes.

[5] The KESS observational array focused on the region around the first quasi-stationary meander crest and trough in the Kuroshio Extension. An array of 46 pressure-sensor-equipped inverted echo sounders (PIES), was centered near  $35^\circ\text{N}$ ,  $146^\circ\text{E}$ , with about 90 km spacing during May 2004–June 2006 [Donohue *et al.*, 2008]. The PIES measured acoustic travel time from the sea floor to the sea surface and  $P_{bot}$ . The PIES Paroscientific quartz  $P_{bot}$  sensor has a stated accuracy of  $\pm 0.01\%$  and 0.1 mbar resolution (Inverted Echo Sounder User's Manual, University of Rhode Island, Narragansett, Rhode Island, 2006, available at <http://www.po.gso.uri.edu/dynamics/IES/index.html>).

<sup>1</sup>Graduate School of Oceanography, University of Rhode Island, Narragansett, Rhode Island, USA.

<sup>2</sup>Department of Physical Oceanography, Woods Hole Oceanographic Institution, Woods Hole, Massachusetts, USA.

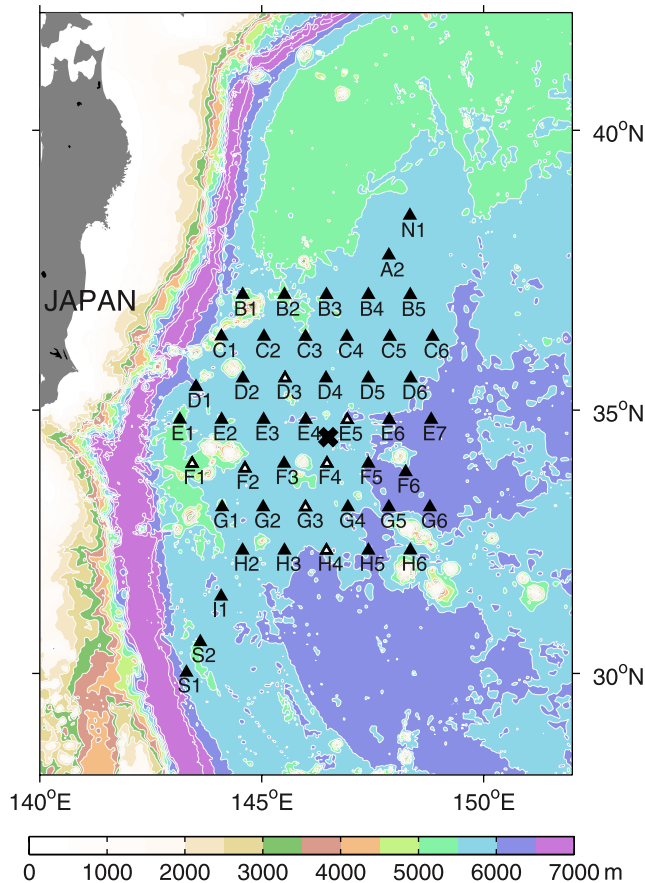


**Figure 1.** KESS array. Triangles indicate PIES sites. Open triangles indicate PIES sites where  $P_{bot}$  measurements ended before September 2005 and these sites were excluded from individual correlation analyses. A cross placed at  $34.5^{\circ}\text{N}$ ,  $146.5^{\circ}\text{E}$  indicates the location of the GRACE estimate that was compared with spatially-averaged in situ  $P_{bot}$ . Bottom topography contoured every 500 m (SRTM30\_PLUS global topography data obtained from Web site [http://topex.ucsd.edu/WWW\\_html/srtm30\\_plus.html](http://topex.ucsd.edu/WWW_html/srtm30_plus.html)).

[6] Ten major tidal constituents were determined and subtracted from each hourly  $P_{bot}$  time series using the response analysis method [Munk and Cartwright, 1966]. Pressure drift was removed using an exponential temporal drift plus a linear trend determined by a least-squares fit. Many PIESs (37 out of 46) were also equipped with RCM-11 current meters moored  $\sim 50$  m above the bottom (CPIES). The bottom current meters determined a stream function at each CPIES site (see Watts et al. [2001] for details).  $P_{bot}$  records converted to stream function were required to match the current-meter-derived estimates, which guided the choice of exponential and linear drift parameters. De-meaned hourly  $P_{bot}$  time series were low-pass filtered with a 72-hour 4th-order Butterworth filter and subsampled at 12-hour increments. Here we report  $P_{bot}$  scaled to equivalent height by dividing each  $P_{bot}$  series by a nominal deep sea density ( $1036 \text{ kg m}^{-3}$ ) and local gravity ( $9.797 \text{ m s}^{-2}$ ). The error in the residual  $P_{bot}$  is estimated as 0.72 cm [Kennelly et al., 2007]. The error in the monthly-averaged residual  $P_{bot}$  is 0.50 cm.

[7] For this comparison study, we produced a spatially-averaged monthly-mean  $P_{bot}$  time series over the observational domain, noted as  $\langle \bar{P}_{bot} \rangle$ . In addition, we also generated monthly-mean  $P_{bot}$  time series ( $\bar{P}_{bot}$ ) for each PIES to compare to GRACE. Measurement durations differed among the PIES sites due to various instrument issues. Seven sites, indicated by open triangles in Figure 1, had  $P_{bot}$  records that ended prior to September 2005 and were excluded from the point-measurement comparisons.

[8] Quantitative comparisons were conducted for the time period November 2004 through June 2006. GRACE was temporarily in a 4-day (61-revolution) repeat cycle during July–October 2004. Due to the lack of global coverage, the monthly GRACE fields have reduced data quality during these months (<http://podaac.jpl.nasa.gov/grace/documentation.html>). GRACE monthly fields are produced based on available data in each month, and some months (May 2004, December 2004, March 2005, June 2005, December 2005, and March 2006) have 1 to 5 missing days. We did not exclude these missing GRACE days when we produced the KESS time averages  $\langle \bar{P}_{bot} \rangle$  and  $\bar{P}_{bot}$ .

### 3. Results

[9] The KESS monthly-array average,  $\langle \bar{P}_{bot} \rangle$ , and GRACE  $P_{bot}$  series, estimated near the center of the KESS domain at  $34.5^{\circ}\text{N}$ ,  $146.5^{\circ}\text{E}$  (cross in Figure 1), track each other and in particular exhibit a consistent seasonal signal (Figure 2). Note the sharp  $P_{bot}$  decrease in winter. This is a basin-scale seasonal cycle of  $P_{bot}$ s related to the seasonal cycle of wind stress change and bottom topography [Gill and Niiler, 1973], and has been observed and simulated previously in the North Pacific [e.g., Bingham and Hughes, 2006]. Differences between the three GRACE products exist. For a given smoothing radius  $R$ , CSR and JPL estimates show higher correlation coefficients ( $Cr \geq 0.74$ ) with  $\langle \bar{P}_{bot} \rangle$  than the GFZ estimates ( $Cr \leq 0.57$ ). All  $Cr$  values are statistically significant within the 95% confidence limit. With increased  $R$  from 300 to 750 km,  $Cr$  values decrease for CSR, 0.82 to 0.74 and GFZ, 0.57 to 0.51. On the other hand, JPL estimates show a small increase of the  $Cr$  from 0.82 to 0.84.

[10] For all three  $R$  comparisons, the root-mean-squared (RMS) differences for JPL estimates show the smallest values of 1.4–1.6 cm (with explained variance of 70–62%), while those for GFZ estimates show the largest values of 2.1–2.3 cm (with explained variance of 32–14%). RMS differences between JPL and CSR differ very little with no apparent relationship to the  $R$  length. The  $Cr$  values and RMS differences demonstrate that GRACE can measure monthly water mass variations of  $\sim 600$ -km scale with high quality in the KESS domain. In addition, CSR and JPL products appear better than GFZ products in the KESS region.

[11] Correlation analysis is also applied between individual in situ KESS  $\bar{P}_{bot}$  and GRACE  $P_{bot}$  at each PIES site, obtained by linear 2-D interpolation from  $1^{\circ}$ -resolution monthly GRACE estimates. The spatial distribution of  $Cr$  shows a distinct spatial structure (Figure 3): high correlation along the northern and western portion of the array. Values larger than 0.6 occur in the northern side of the domain for the CSR and JPL estimates with  $R = 300$  km. This area is

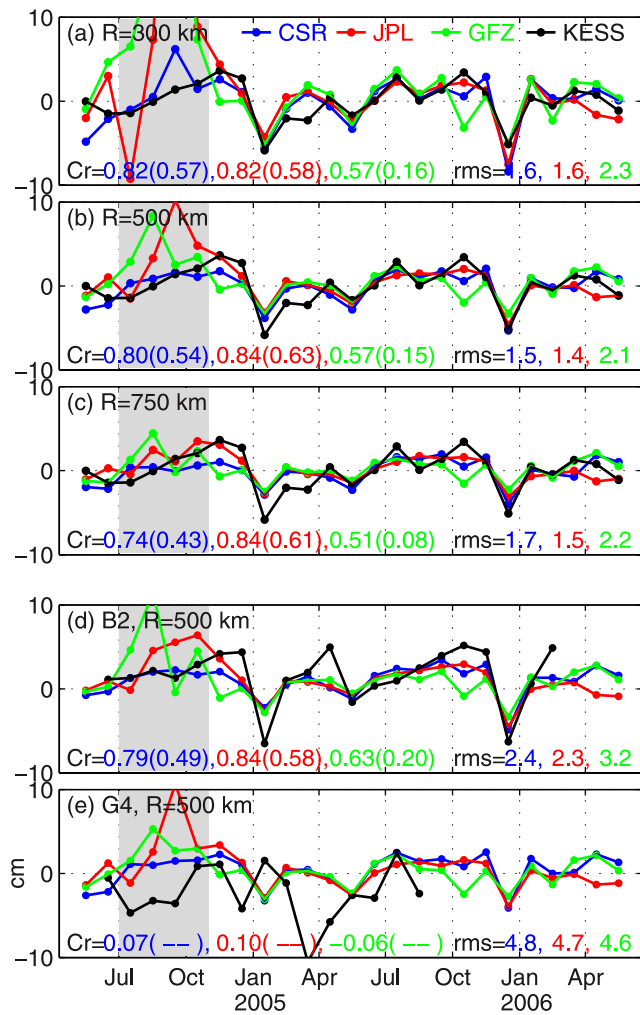


**Figure 2.** Time series of spatially-averaged monthly-mean in situ  $P_{bot}$ ,  $\langle \bar{P}_{bot} \rangle$ , and GRACE  $P_{bot}$  in terms of equivalent water thickness at  $34.5^\circ\text{N}$ ,  $146.5^\circ\text{E}$  with the smoothing radii ( $R$ ) of (a) 300, (b) 500, and (c) 750 km. Time series of individual monthly-mean in situ  $P_{bot}$ ,  $\bar{P}_{bot}$ , and GRACE  $P_{bot}$  at (d) B2 and (e) G4 with  $R = 500$  km. CSR, JPL, and GFZ estimates are represented by blue, red and green, respectively. Gray shaded period indicates July–October 2004 when GRACE estimates were unstable due to the lack of global coverage. Correlation coefficients ( $Cr$ ) and root-mean-squared (RMS) differences are shown respectively at the left bottom and right bottom in each panel (May–October 2004 data were excluded). Lower bounds of the 95% confidence intervals are noted between the brackets. Text color corresponds with line colors CSR (blue) JPL (red), and GFZ (green). Tick marks on x-axis indicate the start of the labeled months.

more elongated northeast-to-southwest direction for the  $R = 500$  and  $750$  km products. Similar to the  $\langle \bar{P}_{bot} \rangle$  comparisons, the GFZ estimates show the lowest  $Cr$ , typically less than 0.6 for all three  $R$  comparisons.

[12] GRACE measurements can potentially determine deep currents through geostrophy. Following a reviewer’s suggestion, we tested correlations between CPIES- and GRACE-derived deep currents. However, we found the

deep currents were not correlated with statistical significance. Since the horizontal scale of seasonal  $P_{bot}$  change is large, the horizontal gradient of  $P_{bot}$  eliminates the dominant seasonal signal, which seems to result in no significant correlations.

[13] KESS  $\bar{P}_{bot}$  measurements near the southeastern area centered at site G4 have almost no correlations with any GRACE products (Figure 3). This low  $Cr$  here is not related to bottom topography because KESS region is located in relatively flat topography. In fact note the relatively high correlations found near seamount complexes adjacent to sites B1-C1-C2 or E2-F2-F1.

[14] Figures 2d and 2e plot the individual monthly time series of in situ  $\bar{P}_{bot}$  and GRACE  $P_{bot}$  with  $R = 500$  km at sites B2 and G4. Site B2 shows good agreement with GRACE  $P_{bot}$ , while site G4 shows poor agreement. Furthermore, the G4  $\bar{P}_{bot}$  seems to contain mesoscale components large enough to obscure the seasonal signal which is prominent in  $\langle \bar{P}_{bot} \rangle$ .

[15] We can compute spatial correlations between PIESS to determine a domain-wide distribution of characteristic length scale, unlike the above-mentioned previous GRACE evaluation studies using pointwise  $P_{bot}$  measurements. At each PIESS we computed spatial correlations between all  $P_{bot}$

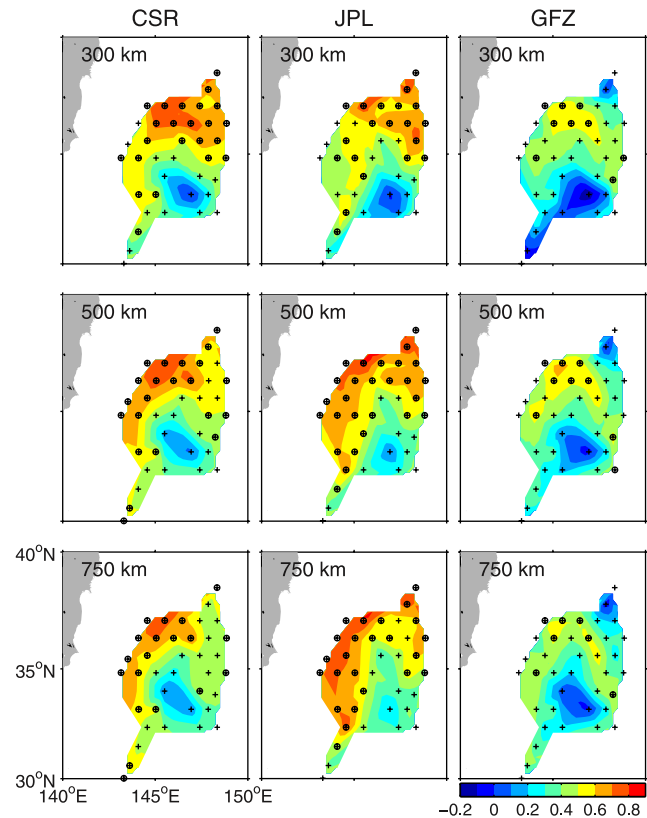


**Figure 3.** Correlation maps between KESS  $\bar{P}_{bot}$  and GRACE measurements. The columns represent correlation maps for (left) CSR, (middle) JPL, and (right) GFZ GRACE estimates, and the rows represent the smoothing radii of (top) 300, (middle) 500, and (bottom) 750 km. Pluses indicate PIESS sites used in correlation calculations. Pluses with circles indicate sites where the  $Cr$  values are significant within the 95% confidence limit.

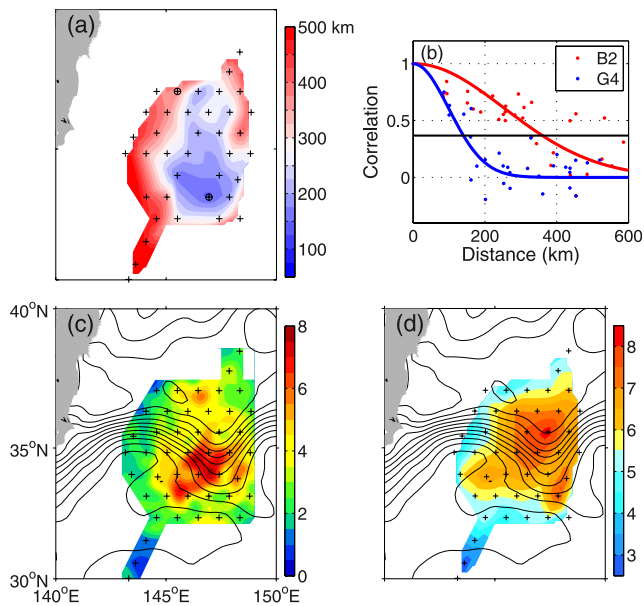


**Figure 4.** (a) Spatial correlation length scale map computed from in situ  $P_{bot}$  measurements. (b) Spatial correlations at sites B2 (red) and G4 (blue) superimposed by Gaussian fitted curves computed using all available in situ  $P_{bot}$  measurements. Horizontal line indicates e-folding correlation length. (c) Colored contour map of eddy kinetic energy ( $\times 10^{-3} \text{ m}^2 \text{ s}^{-2}$ ) computed using optimally-interpolated deep current fields. (d) Colored contour map of RMS  $P_{bot}$  (cm). Contours superimposed on Figures 4c and 4d indicate mean dynamic topography during the KESS period from satellite altimetry. Contour intervals are 10 cm. Pluses in Figures 4a, 4c, and 4d indicate PIES sites used for calculations. Pluses with circles in Figure 4a indicate the two sites B2 and G4.

pairs, and then those were least-squares-fitted to a Gaussian curve  $G(r) = e^{(-r/r_0)^2}$ , where spatial lag  $r$  is horizontal distance and  $r_0$  is e-folding scale fit to the spatial correlations. A clear spatial structure emerges. Figure 4a maps the  $r_0$  values computed at each PIES site (recall that we excluded 7 short PIES records). The western and northeastern areas have long  $r_0$  values ( $>300$  km), while the middle area of northern half and southeastern area have short  $r_0$  values ( $<300$  km). Site G4 has the shortest  $r_0$  of 140 km. Two correlation functions are shown for the two extrema in the spatial correlation in Figure 4b. Site B2 exhibits high correlations with many PIES sites in the array, while site G4 shows a quick drop of correlations when the distances become longer than about 150 km.

[16] A region of high eddy kinetic energy (EKE) coincides with the region of short  $r_0$ . We computed EKE using optimally interpolated (OI) deep current maps (Figure 4c). OI maps are constructed with a 100 km Gaussian correlation function and the OI grid has 10-km resolution. Short-wavelength  $P_{bot}$  components, small  $r_0$ , are closely associated with deep mesoscale eddies energetic under the first quasi-stationary meander trough of the Kuroshio Extension, where the RMS variability of  $P_{bot}$  is large (Figure 4d). The  $r_0$  and EKE maps show a remarkably similar pattern to the  $Cr$  maps in Figure 3. Low  $Cr$  area coincides with short  $r_0$ /

high EKE area and high  $Cr$  area coincide with long  $r_0$ /low EKE area. This result demonstrates that short-wavelength mesoscale  $P_{bot}$  components in the KESS region cause low correlation between in situ  $\bar{P}_{bot}$  and GRACE  $P_{bot}$ .

#### 4. Conclusion

[17] Due to the lack of available  $P_{bot}$  measurements, all previous validations of GRACE in the ocean have used pointwise in situ  $P_{bot}$  measurements for the comparisons. This study compared in situ  $P_{bot}$  measurements from a wide array covering  $600 \text{ km} \times 600 \text{ km}$  area with GRACE  $P_{bot}$  estimates in the Kuroshio Extension. Domain-averaged in situ  $P_{bot}$  measurements,  $\langle \bar{P}_{bot} \rangle$ , revealed good agreement with the GRACE  $P_{bot}$  estimates from both CSR and JPL gravity products, and relatively poor agreement with those from GFZ. The large-scale seasonal cycle dominates the monthly and spatially averaged mass variability in this region [Bingham and Hughes, 2006]. The correlation analyses with  $\langle \bar{P}_{bot} \rangle$  was insensitive to the choice of  $R$  length (300–750 km) applied to GRACE estimates. This study demonstrates that GRACE mission yields high-quality large-scale averages of monthly-mean  $P_{bot}$  fluctuations in the Kuroshio Extension region.

[18] Individual comparisons between in situ  $\bar{P}_{bot}$  and GRACE estimates at each PIES site reveal a spatially-varying pattern of correlations. Munekane [2007] shows that pointwise  $P_{bot}$  and GRACE estimates may differ due to two factors—artificial leakage from the mass variations on land and filtering of short spatial-scale oceanographic components. From our  $P_{bot}$  array measurements, we show that when short-wavelength mesoscale  $P_{bot}$  components dominance the monthly-averaged records, the comparisons between pointwise in situ  $P_{bot}$  measurements and GRACE estimates can result in low correlations.

[19] **Acknowledgments.** GRACE data were processed by D. P. Chambers, supported by the NASA Earth Science REASON GRACE Project, and are available at <http://grace.jpl.nasa.gov>. We thank Karen Tracey, Maureen Kennelly, and Andrew Greene for their great help in processing the KESS data. Thanks are given also to two anonymous reviewers for their helpful suggestions. This work was supported by NSF grant OCE-0221008.

#### References

- Bingham, R. J., and C. W. Hughes (2006), Observing seasonal bottom pressure variability in the North Pacific with GRACE, *Geophys. Res. Lett.*, **33**, L08607, doi:10.1029/2005GL025489.
- Chambers, D. P. (2006a), Evaluation of new GRACE time-variable gravity data over the ocean, *Geophys. Res. Lett.*, **33**, L17603, doi:10.1029/2006GL027296.
- Chambers, D. P. (2006b), Observing seasonal steric sea level variation with GRACE and satellite altimetry, *J. Geophys. Res.*, **111**, C03010, doi:10.1029/2005JC002914.
- Donohue, K. A., et al. (2008), Program studies the Kuroshio Extension, *EOS Trans. AGU*, **89**(17), 161–162.
- Gill, A., and P. Niiler (1973), The theory of seasonal variability in the ocean, *Deep Sea Res.*, **20**, 141–177.
- Jayne, S. R., J. M. Wahr, and F. O. Bryan (2003), Observing ocean heat content using satellite gravity and altimetry, *J. Geophys. Res.*, **108**(C2), 3031, doi:10.1029/2002JC001619.
- Kanzow, T., F. Flechtner, A. Chave, R. Schmidt, P. Schwintzer, and U. Send (2005), Seasonal variation of ocean bottom pressure derived from Gravity Recovery and Climate Experiment (GRACE): Local validation and global patterns, *J. Geophys. Res.*, **110**, C09001, doi:10.1029/2004JC002772.
- Kennelly, M., K. L. Tracey, and D. R. Watts (2007), Inverted echo sounder data processing manual, *GSO Tech. Rep. 2007-02*, Grad. Sch. of Oceanogr., Univ. of R. I., Narragansett. (Available at [http://www.po.gso.uri.edu/dynamics/publications/tech\\_rpts/IESprocessman.pdf](http://www.po.gso.uri.edu/dynamics/publications/tech_rpts/IESprocessman.pdf))

- Munekane, H. (2007), Ocean mass variations from GRACE and tsunami gauges, *J. Geophys. Res.*, *112*, B07403, doi:10.1029/2006JB004618.
- Munk, W. H., and D. E. Cartwright (1966), Tidal spectroscopy and prediction, *Philos. Trans. R. Soc. London, Ser. A*, *259*, 533–581.
- Rietbroek, R., P. LeGrand, B. Wouters, J.-M. Lemoine, G. Ramillien, and C. W. Hughes (2006), Comparison of in situ bottom pressure data with GRACE gravimetry in the Crozet-Kerguelen region, *Geophys. Res. Lett.*, *33*, L21601, doi:10.1029/2006GL027452.
- Tapley, B. D., S. Bettadpur, J. C. Ries, P. F. Thompson, and M. Watkins (2004), GRACE measurements of mass variability in the Earth system, *Science*, *305*, 503–505.
- Watts, D. R., X. Qian, and K. L. Tracey (2001), On mapping abyssal current and pressure fields under the meandering Gulf Stream, *J. Atmos. Oceanic Technol.*, *18*, 1052–1067.
- 
- K. A. Donohue, J.-H. Park, and D. R. Watts, Graduate School of Oceanography, University of Rhode Island, Narragansett, RI 02881, USA. (jpark@gso.uri.edu)
- S. R. Jayne, Department of Physical Oceanography, Woods Hole Oceanographic Institution, Clark 313A, MS 21 Woods Hole, MA 02543, USA.